Journal of Applied Polymer Science

Concentration effect on aggregation and dissolution behavior of poly(*N*-isopropylacrylamide) in water

Yongbin Yan,[1] Lianghui Huang,[2] Quan Zhang,[1] Hu Zhou[3]

[1]Hubei Key Laboratory of Biomass-Resource Chemistry and Environmental Biotechnology, Hubei Engineering University, Xiaogan 432000, People's Republic of China

[2]Guangdong Nanhai ETEB Technology Co., Ltd., Foshan 528251, People's Republic of China

[3]School of Materials Science and Engineering, Wuhan Textile University, Wuhan 430200, People's Republic of China

Correspondence to: H. Zhou (E-mail: zhouhu2007@gmail.com)

ABSTRACT: The concentration effect on aggregation and dissolution behavior of poly(*N*-isopropylacrylamide) (PNIPAM) in water was studied. Three concentration regimes with different phase behavior were identified by differential scanning calorimetry (DSC). Further optical, light-scattering, and rheological studies indicated that the appearance of different regimes arose from their corresponding solution structures below lower critical solution temperature (LCST): free chains and small clusters in regime I, large clusters in regime II, and a gel-like network in regime III. Different solution structures below LCST led to different phase-separated patterns formed above LCST: colloidal particles in regime I, large precipitate in regime II, and the sponge-like solid in regime III, which was well understood based on the overlapping parameter P. Different phase-separated patterns therefore resulted in different remixing behavior as observed by DSC. This work suggests that the swelling and collapse behavior of PNIPAM based hydrogels was controlled through the design of their phase-separated patterns, and therefore provided a way to develop high performance thermo-sensitive materials. © 2014 Wiley Periodicals, Inc. J. Appl. Polym. Sci. **2015**, *132*, 41669.

KEYWORDS: polyamides; phase behavior; stimuli-sensitive polymers; functionalization of polymers

Received 18 June 2014; accepted 22 October 2014

DOI: 10.1002/app.41669

INTRODUCTION

The thermally induced phase behavior of poly(*N*-isopropylacrylamide) (PNIPAM) in aqueous media has attracted much more interests nowadays since this polymer can exhibit a well-defined lower critical solution temperature (LCST) in water.[1–3] Below LCST, PNIPAM exists in an expanded conformation in water to form a homogeneous solution. It becomes more compact above LCST, which results in the formation of the separated liquid and solid phases. PNIPAM therefore exhibits potential applications as a thermo-sensitive polymer,[1–3] especially when copolymerized with other monomers to control the rheological properties of gels and solutions.[4–6]

The phase behavior of a single PNIPAM chain in water was first investigated by Wu *et al.*[7–9] They found that the swelling and collapse of a single chain in water were not all-or-none processes: four distinct states including the coil, the crumpled coil, the molten globule, and the globule could be identified. The effect of chain overlapping on the transition behavior of PNIPAM has also been studied by rheology,[10] dynamic, and static light scattering,[11] nuclear magnetic resonance (NMR),[12] and microcalorimetry.[13,14] These investigations suggested that the aggregation and dissolution of PNIPAM chains in nondilute solutions were also multi-stage processes. For example, the dissolution of aggregated chains involved two processes, presumably, the disruption of additional hydrogen bonds formed in the collapsed state and the dissolution of the collapsed and entangled chains.[13]

This thermally induced phase transition is generally thought to be the results of the hydrophobic associations between the isopropyl groups and the disruption of hydrogen bonds between the amide groups and water above LCST. Recently, Bischofberger *et al.* used microcalorimetry to study correlations between solvent and PNIPAM solution thermodynamics.[15] Through the addition of an organic solute classified as kosmotrope in water, they found that the phase transitions of PNIAPM evolved relative to the solvent composition at which the excess mixing enthalpy of the solvent mixtures became minimal. Their studies showed that hydrophobic hydration was the dominant contribution governing the phase behavior of PNIPAM, which was strongly determined by the mean energetics of the aqueous medium.

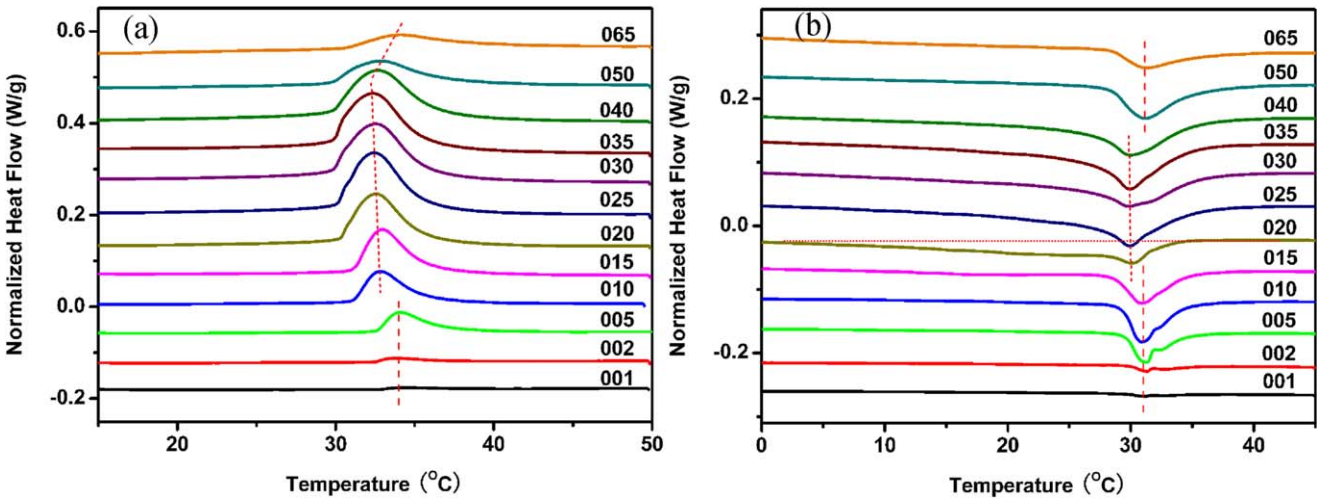

Figure 1. DSC curves of heating run (a) and subsequent cooling run (b) for different PNIPAM aqueous solutions. [Color figure can be viewed in the online issue, which is available at wileyonlinelibrary.com.]

However, studies on the phase behavior of PNIPAM in nondilute solutions are still limited, especially on its concentration dependence which is closely related to the chain overlapping and entanglement. For nondilute solutions, one main obstacle is that aggregation usually leads to precipitation, which makes the characterization difficult and irreproducible. In our work, concentration effect on the phase transition of PNIPAM was explored using a variety of testing techniques. Our studies found that the aggregation and dissolution behavior of PNIPAM in water strongly depended on the solution structures below LCST.

EXPERIMENTAL

Materials

N-isopropylacrylamide (NIPAM) was purchased from Tokyo Kasei Kogyo Co. (Tokyo, Japan). Azobisisobutyronitrile (AIBN), tetrahydrofuran (THF), and diethyl ether were from Sigma Co. All the reagents were purified and dried before use.

Preparation of PNIPAM Aqueous Solutions

PNIPAM was synthesized via free-radical polymerization in THF with AIBN as initiator. Firstly, the stock solution of NIPAM (1.50 mol) and AIBN (1.55 mmol) in THF (20.00 mL) was prepared and deoxygenated by three freeze-evacuate-thaw cycles. Then, polymerization was carried out at 60°C for 15 h under nitrogen atmosphere. The product was precipitated in excess diethyl ether. The obtained polymers were purified by three dissolve-precipitate cycles. The molecular weight (M_w) and polydispersity index (M_w/M_n) of PNIPAM by gel permeation chromatography (GPC) were 1.92×10^4 /mol and 1.50, respectively, using THF as mobile phase and polystyrene as standards.

PNIPAM was dissolved in distilled water to prepare a series of PNIPAM aqueous solutions with the concentration of 1.0, 2.0, 5.0, 10.0, 15.0, 20.0, 25.0, 30.0, 35.0, 40.0, 50.0, and 65.0 wt %, which were labeled as 001, 002, 005, 010, 015, 020, 025, 030, 035, 040, 050, and 065, respectively. To keep them in equilibrium, all the solutions were rested for 1 week at room temperature before being used.

Measurements

The thermal transition behavior of PNIPAM aqueous solutions was measured on a Mettler-Toledo differential scanning calorimeter (DSC) under nitrogen, which was calibrated with a standard indium sample. For all the measurements, about 10 mg of PNIPAM aqueous solutions were hermetically sealed in a 40 μL aluminum pan, and the reference aluminum pan was kept empty. In the standard scanning procedure, the heating run was conducted from 10 to 50°C at 3°C/min, followed by 3 min equilibrium, and subsequently the cooling run was carried out down to 0°C with the same rate.

Optical microscopy images were obtained on a Nikon MM-400/L measuring microscope. About 1 mL PNIPAM aqueous solutions were hermetically sealed in a glass guide channel, and then the phase-separated patterns were generated through heating the sample solutions at 3°C/min above LCST as the DSC test. The sample solutions were open at 50°C for drying. All optical images with optimal quality were recorded after the completion of water evaporation.

Dynamic light scattering (DLS) was done on Zetasizer Nano ZS, for which noninvasive back scatter technology was applied. A He/Ne laser (wavelength: 632.8 nm) was selected, and laser output power was attenuated to the desired values (4 mW). About 1 mL aqueous solutions was dropped very slowly into the sample cell. Then, the sample cell rested for 60 min at room temperature. The data were collected with a temperature increment of 2°C (accuracy: 0.1°C). The heating rate was 1°C/min and the equilibrium time was 5 min.

Rheological tests were performed on a Physica MCR 301 rheometer equipped with a 50 mm diameter cone plate set 0.054 mm apart at 15 C. Strain amplitude (γ) sweeps were conducted at angular frequencies (ω) of 1 and 10 rad/s in the overall amplitude range of 1–100%, which determined the linear viscoelastic range and the structural strength of solutions.

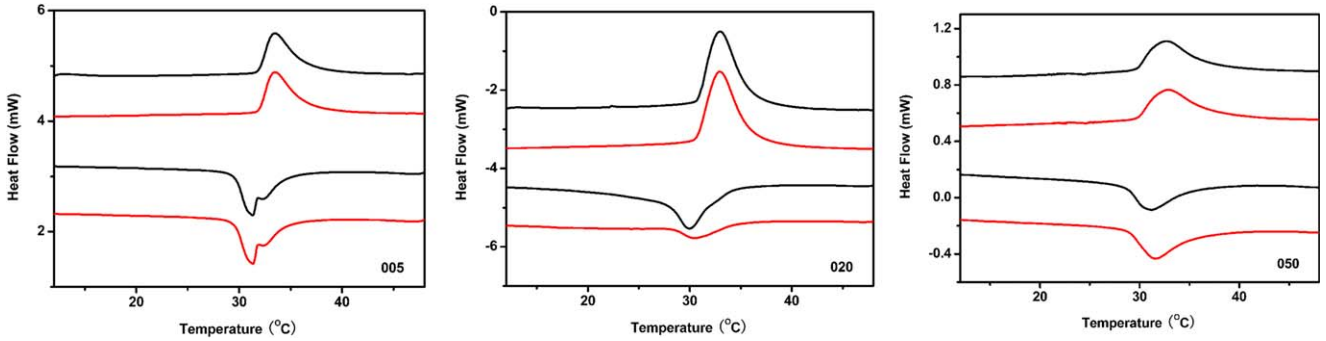

Figure 2. DSC curves of multi heating–cooling cycles for different PNIPAM aqueous solutions (black lines: the 1st heating–cooling cycles. Red lines: the 2nd heating–cooling cycles. The heating and cooling rates were both 3°C/min). [Color figure can be viewed in the online issue, which is available at wileyonlinelibrary.com.]

Dynamic frequency (ω) sweeps were done at strain amplitude (γ) of 2% in the angular frequency range of 0.1–100 rad/s. All measurements were made at frequencies that led to linear responses. All samples rested for 24 h at 15°C before tests.

RESULTS AND DISCUSSION

DSC Analysis

The concentration dependence of demixing and dissolution behavior of PNIPAM in water was shown in Figure 1. Three main concentration regimes were identified according to their demixing and dissolution behavior. Clearly the thresholds between two regimes were not sharp since they would change slightly in the heating and cooling runs. It was just like the crossover regions between two regimes, but our discussions are not influenced.

In regime I where the upper threshold was ca. 10 wt %, the demixing peak at 34.1°C was observed in the heating run, and two remixing peaks at 32.5 and 31.0°C, respectively, were found in the cooling run. Multi heating-cooling cycles with the same rate were applied to evaluate their stabilities (Figure 2). The results showed an excellent consistency, which indicated that the aggregation and precipitation had no evident effect. The scanning rate dependence was also examined (Figure 3). The demixing peak slightly shifted to higher temperature with the heating rates increasing. Ding and Zhang suggested that the chain association lagged behind the temperature change, which resulted in this shift.[13,14] The remixing peak around 32.5°C was always present in all the cooling run, and the remixing peak around 31.5°C became clearly asymmetrical as the heating and cooling rates decreased. For example, for the heating–cooling cycle, where the heating and cooling rates were 1 and 3°C/min, respectively, at least three peaks could be identified in the cooling run after the deconvolution of the cooling curve [Figure 3(c)]. Two peaks at the lower temperature were highly in agreement with the results reported by Zhang *et al.*,[13,14] which suggested that they possibly came from the disruption of the additional hydrogen bonds and the dissolution of the collapsed chains, respectively.

In regime II, where the upper threshold was ca. 40 wt %, the temperature of demixing peak in the heating run decreased from 32.8 to 32.4°C with increasing polymer concentration, whereas the temperature of dissolution peak was nearly invariable, ca. 29.9°C in the cooling run. Interestingly, the marked streaking effect, also large supercooling, occurred in the cooling run. Moreover, this streaking effect became more serious in multiheating–cooling cycles (Figure 2). The presence of large supercooling was hardly influenced by the scanning rates (e.g., in the range 1–10°C/min).

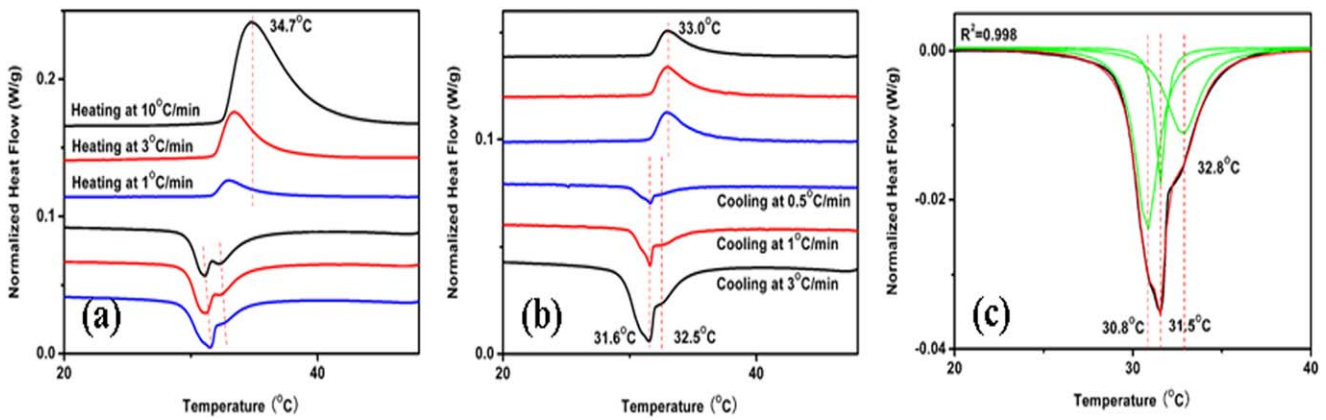

Figure 3. DSC curves with different heating or cooling rate for 5.0 wt % PNIPAM aqueous solution. (a) The cooling rate was 3°C/min. (b) The heating rate was 1°C/min. (c) The deconvolution of the cooling curve at the heating and cooling rates of 1 and 3°C/min, respectively. [Color figure can be viewed in the online issue, which is available at wileyonlinelibrary.com.]

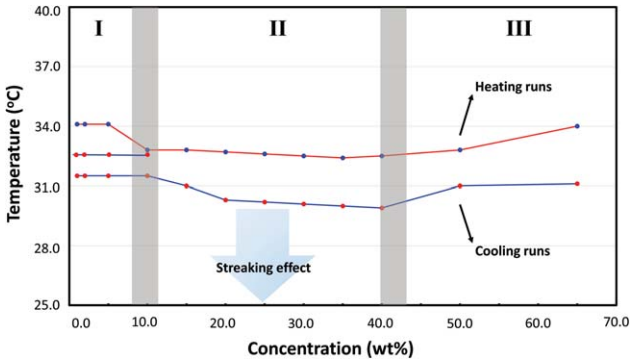

Figure 4. Thermal transition temperatures of the PNIPAM aqueous solutions with different concentrations from DSC in the heating and cooling scans. [Color figure can be viewed in the online issue, which is available at wileyonlinelibrary.com.]

In regime III where the polymer concentration was beyond 40 wt %, the temperature of demixing peak was increased in the heating run, while the temperature of dissolution peak was nearly invariable, ca. 31.1°C in the cooling run. Importantly, the streaking effect was not observed during the cooling process. The perceived streaking effect was not yet found in multi heating–cooling cycles, and their demixing and dissolution behavior hardly changed in the cycles (Figure 2). This was completely different from the phase behavior in regime II, where the streaking effect was always present in the cooling run. All the DSC data of the PNIPAM aqueous solutions were summarized in the peak temperature vs concentration phase diagram (Figure 4). The results showed that three regimes were clearly identified although the phase transition was not sharp.

Optical Observation

Figure 5 exhibited typical phase-separated patterns formed above LCST. All the PNIPAM solutions were found to show a milk-white appearance above their LCST. In regime I, the colloidal suspensions were generally formed above LCST, which were kept stable at least for 1 h. For example, it was shown that 1–3 μm colloidal particles were formed for 5.0 wt % PNIPAM in Figure 5, which was in good agreement with later DLS results. Such an unusual stability was reported previously for the phase separation of extremely dilute solutions (<0.05 wt %).[16] It was suggested that PNIPAM colloids were stabilized by charges born of the chain end groups[17] or the hydrated hydrophilic groups survived above the LCST.[18] In regime II, the suspensions were very unstable above LCST, and the precipitation occurred quickly. The dried precipitates typically showed the appearance of a bulk solid. For example, crack was induced by drying shrinkage for 20.0 wt % PNIPAM in Figure 5. In regime III, the whole PNIPAM solutions became a milk-white bulk solid above LCST. Similar results were reported for linear[6] and branched[19] block copolymers of acrylamide (AM) and NIPAM. The dried bulk solids were found to be highly porous, like a sponge structure, e.g., for 50.0 wt % PNIPAM in Figure 5.

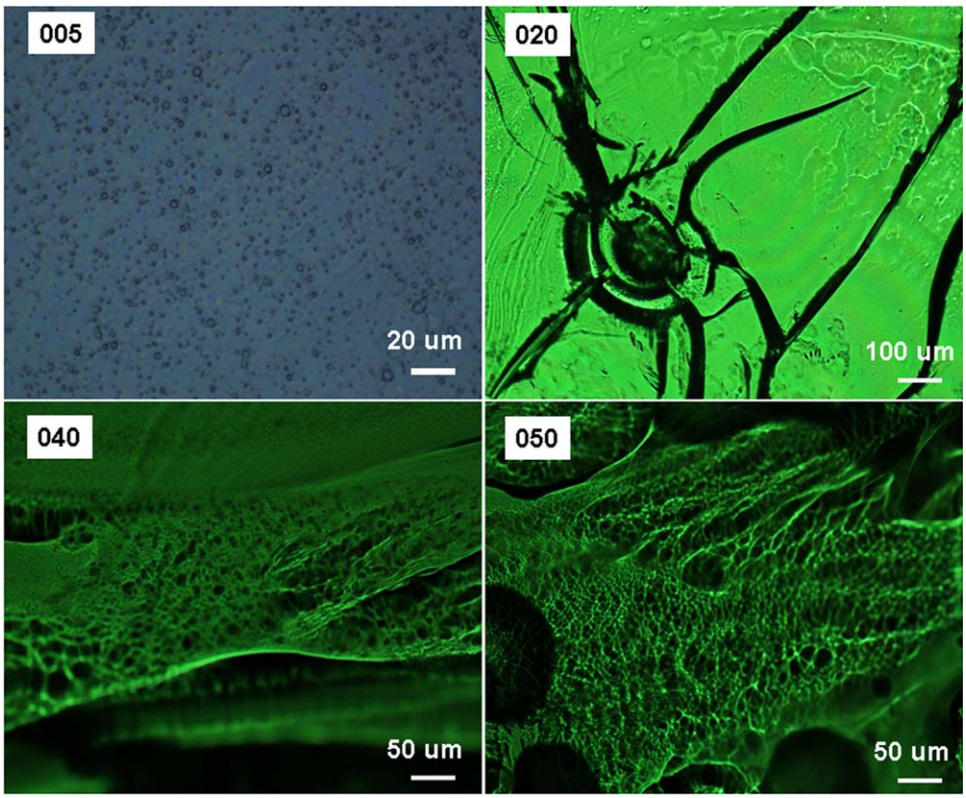

Figure 5. Optical microscopy images of the phase-separated patterns formed above LCST. [Color figure can be viewed in the online issue, which is available at wileyonlinelibrary.com.]

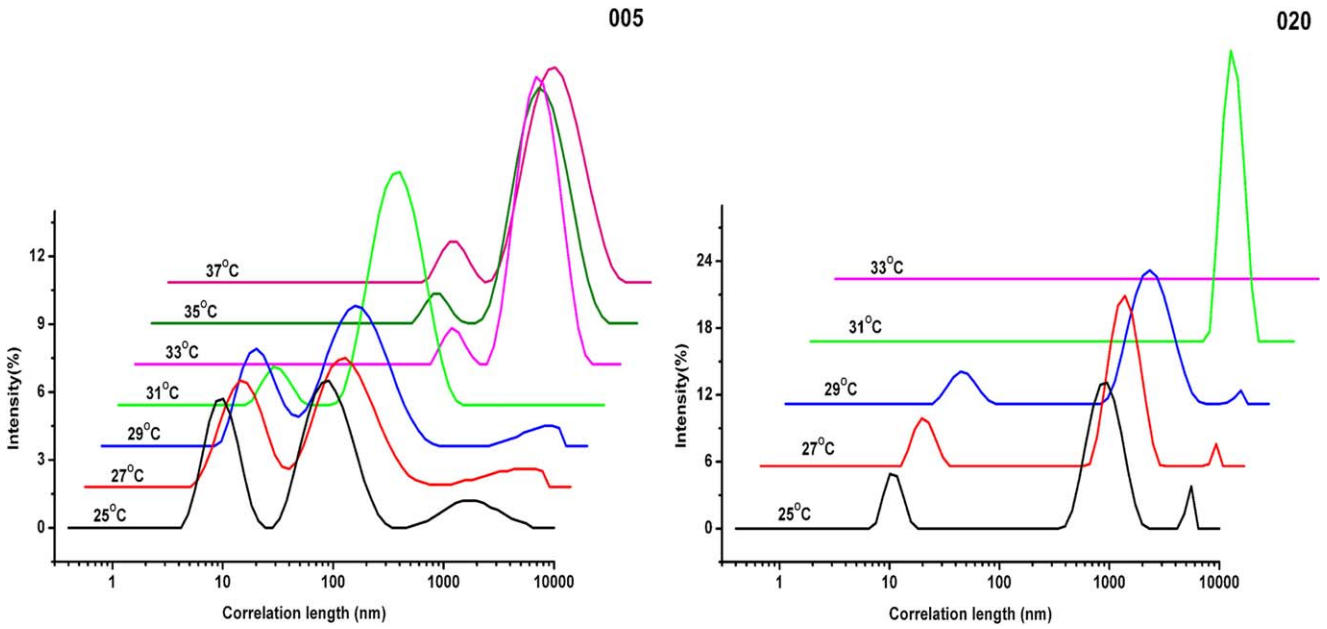

Figure 6. DLS correlation length distribution of 5.0 and 20.0 wt % PNIPAM solutions at different temperatures. [Color figure can be viewed in the online issue, which is available at wileyonlinelibrary.com.]

DLS Study

Dynamic light scattering (DLS) was used to follow the demixing process of the PNIPAM aqueous solutions. Figure 6 showed light scattering data of 5.0 and 20.0 wt % PNIPAM solutions recorded at different temperatures.

Below LCST, both PNIPAM solutions showed a characteristic multimodal distribution. The first component located at around 10 nm was attributed to the free PNIPAM chains. The other two components should be associated with interchain clustering of PNIPAM chains. Through DLS, Yu *et al.* found two correlation length modes in 5.0 wt % PNIPAM ($M_w = 3.22 \times 10^5$ g/mol) aqueous solutions below LCST.[20] Pamies *et al.* also observed the bimodal structure (one with 2–3 nm and the other with ~100 nm) at 1.0 wt % polymer concentration for lower molecular weight PNIPAM samples ($M_w = 5.35 \times 10^3$ g/mol, $M_w/M_n = 1.13$; $M_w = 9.01 \times 10^3$ g/mol, $M_w/M_n = 1.12$).[21] However, they could not extract a fast relaxation mode in 1.0 wt % PNIPAM aqueous solutions ($M_w = 1.34 \times 10^4$ g/mol, $M_w/M_n = 1.12$). They thought that the weaker fast relaxation mode was influenced by the stronger signals produced from the large aggregates. These studies indicated that the peak at 100–300 nm surely corresponded to the PNIPAM clusters in water. Since the topological entanglement between chains would not take place because of the relatively low molecular weight of PNIPAM here,[22] this clustering should arise from the hydrophobic associations between the isopropyl groups or the formation of hydrogen bonds between PNIPAM chains. Notably, the cluster size increased with the increase of PNIPAM concentration below LCST. One huge cluster spanning the whole space would be expected when the PNIPAM concentration was high enough. In this way, a network structure would occur in the solutions.

Above LCST, the peaks of component representing the free polymer chains disappeared, which indicated that individual chains associated into multichain aggregates. Interestingly, the characteristic bimodal distribution occurred for 5.0 wt % PNIPAM. This was different from the results reported by Balu *et al.* that high molecular weight of PNIPAM ($M_w = 1.4 \times 10^5$ g/mol, concentration: 1–6 wt %) associated into the uniform multichain aggregates above LCST.[23] This difference should be ascribed to the topological entanglement occurred for PNIPAM with high molecular weight. For 20.0 wt % PNIPAM, no peaks were shown above LCST, which suggested further aggregation and flocculation. This was supported by the above optical observation.

Rheological Study

Rheological method is applicable for identifying the formation of gel-like network in the solutions, and hence the rheological study was carried out for PNIPAM aqueous solutions. The typical rheological results were shown in Figure 7 for the PNIPAM solutions at different concentrations.

The frequency sweeps were undertaken on 20.0, 30.0, and 40.0 wt % PNIPAM solutions below LCST [Figure 7(a)]. Notably, three samples deviated from the classic Maxwell model of $G' \propto \omega^2$ and $G'' \propto \omega^1$ in the terminal regime. Especially for 40.0 wt % PNIPAM solution, G' and G'' had the same power-law exponent in the terminal regime, $G' \sim G'' \sim \omega^{0.83}$. This suggested the formation of a gel-like structure for 40.0 wt % PNIPAM solution. Previous rheological investigations found that the systems near the gel point exhibited simple relaxation behavior, where G' and G'' obeyed a scaling law with the same exponent.[24,25] For 20.0 and 30.0 wt % PNIPAM solutions, their frequency dependence suggested being far from the gel point. Moreover, the structural strength of the solutions was characterized through the strain sweeps at different frequencies [Figure 7(b)], which was important for the formation of phase-separated patterns.[26] The 20.0 and 30.0 wt % PNIPAM solutions exhibited a very small G', lower

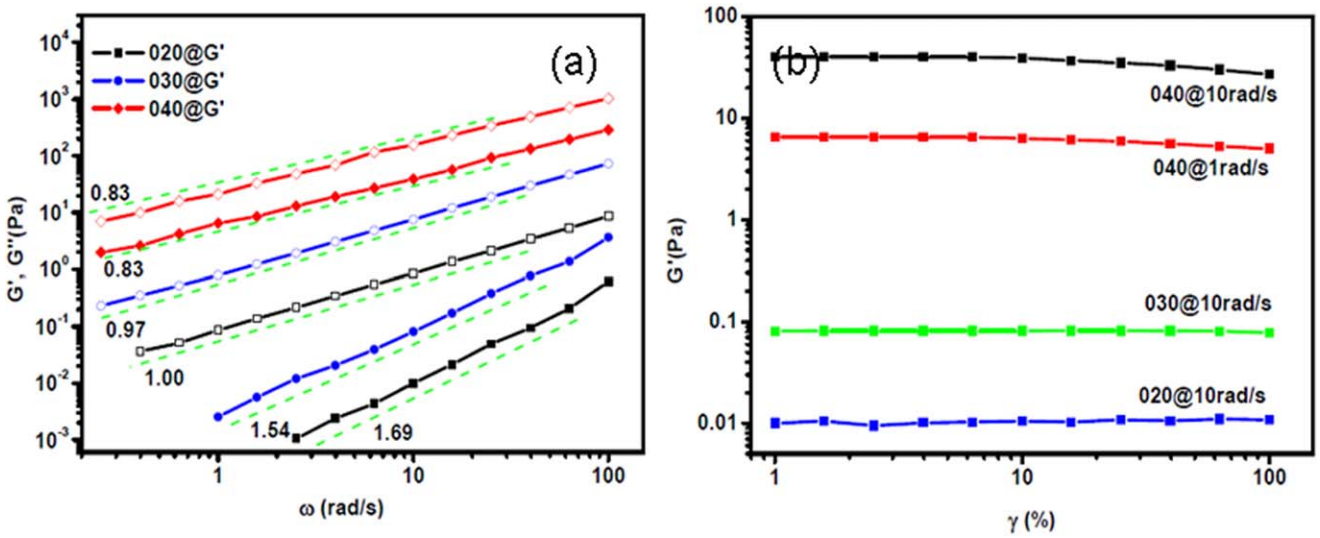

Figure 7. Storage modulus (G') and loss modulus (G'') of different PNIPAM aqueous solutions as functions of angular frequency (ω) and strain amplitude (γ) at 15°C. (a) The strain amplitudes (γ) was 2%; (b) the angular frequency (ω) were 1 and 10 rad/s. [Color figure can be viewed in the online issue, which is available at wileyonlinelibrary.com.]

than 0.1 Pa, while 40.0 wt % PNIPAM solution showed an unusual large G', much higher than 1 Pa, which was due to the formation of a gel-like solution structure.

Concentration Effect

As demonstrated above, the demixing and dissolution behavior of PNIPAM aqueous solutions showed the strong concentration effect. Their phase behavior was summarized in Figure 8, where the upper coils are PNIPAM chains below LCST, and the lower images are the phase-separated patterns formed above LCST. Three distinct regimes were observed, where different phase-separated patterns were generated above LCST, and correspondingly caused different remixing behavior. Our above studies showed that PNIPAM aqueous solutions below LCST changed from a simple solution to a gel with the increase of polymer concentration. Intuitively, the appearance of different regimes should strongly depend on their corresponding solution structures.

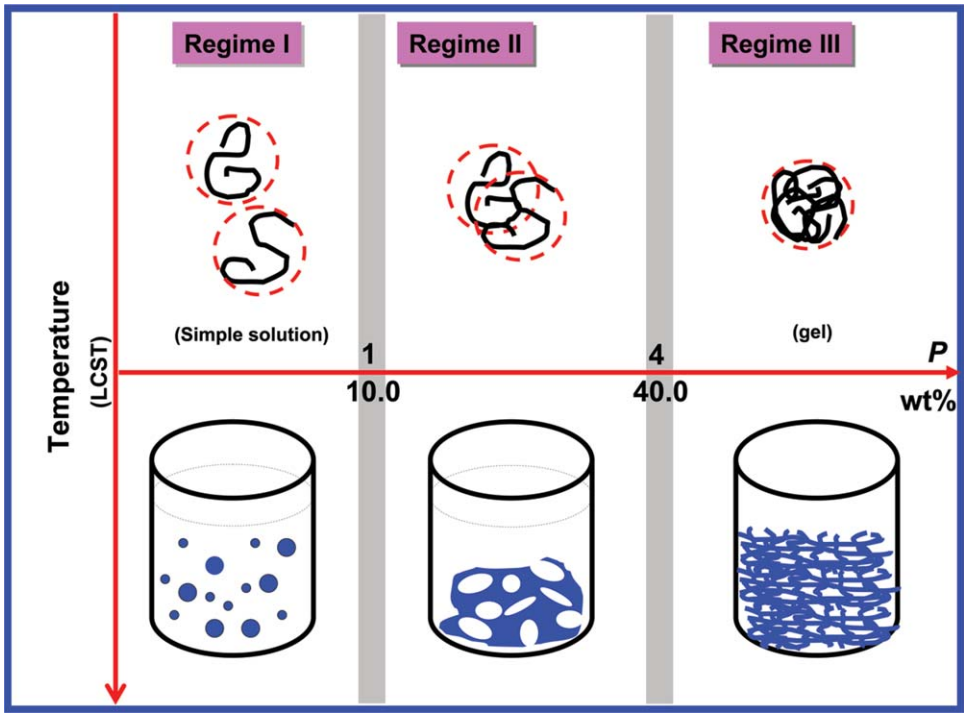

Figure 8. Schematic of the aggregation and dissolution behavior of PNIPAM chains in water. [Color figure can be viewed in the online issue, which is available at wileyonlinelibrary.com.]

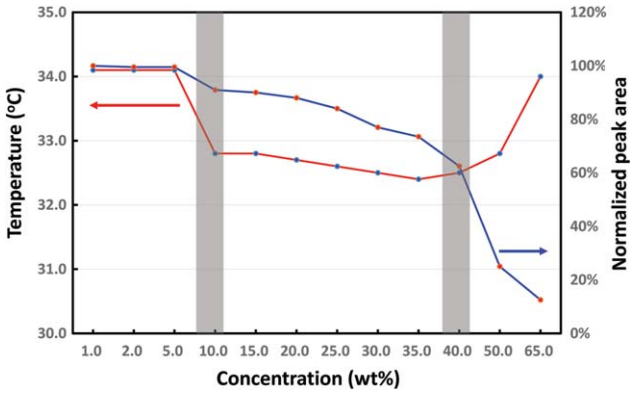

Figure 9. Peak temperature and normalized peak area of different PNIPAM aqueous solutions obtained from DSC in the heating run. [Color figure can be viewed in the online issue, which is available at wileyonlinelibrary.com.]

To help to understand the solution structure, one overlapping parameter, *P*, was introduced (*eq.* 1),[22]

$$P=\frac{\phi R^3}{Nb^3}=\phi N^{0.5} \quad (1)$$

Where φ was the polymer volume fraction, R was the coil size, N was the polymerization degree (ca.100 here), and b was the monomer size. The overlapping parameter P, therefore quantified the number of chains in an expanded volume of coils. Figure 8 showed the P values of the PNIPAM solutions. The two thresholds were found to get $P \sim 1$ and $P \sim 4$, respectively. Notably, the interchain association should strongly depend on their high overlap. Thus the P values suggested the underlying reason that caused different phase-separated regimes.

In regime I, the free chains and the small clusters were present below LCST, as evidenced by the above DLS results. Since $P<1$ (which means that the PNIPAM solutions was in the dilute regime), the weak interchain interaction did not contribute to the formation of the network below LCST. As a result, intrachain contraction and interchain association led to the form of colloidal particles above LCST. The bimodal size distribution of colloidal particles (observed by DLS in Figure 6) probably arose from the intensive concentration fluctuation that was always present in the $P<1$ polymer solutions.[22] For this reason, the bimodal remixing behavior (observed by DSC in Figure 1) was well explained, and the remixing shoulder at 32.5°C was from the melting of nanoscale particles, while the peak at 31.0°C was from the melting of microscale particles. It was assumed that the nanoscale particles were dissolved more easily, which was imputable to large surface/volume ratio compared with the macroscale particles. Recent light-scattering study on the melting of a single-chain PNIPAM globule revealed that the outer shell of the globule melted faster than the inner core of the globule.[8]

In regime II, the gel-like structure was not formed below LCST although the large clusters were present, which was supported by the above DLS and rheological studies. This was due to the medium chain overlapping ($1<P<4$), which caused that regime II was still far from the gel point. Although the gel was possibly formed above LCST due to the interchain association, the connectivity [the structural strength of the solutions was very low as shown in Figure 7(b)] did not allow uniform shrinkage because the self-generated stress led to mechanical fracture and collapse of network.[26,27] Finally, the large precipitates were achieved, as shown in Figure 5. The streaking effect was assumed to be the result of the large precipitates, because they dissolved more slowly as suggested by Wu and Zhou.[8]

In regime III, the mean-field prediction was applicable because of high overlapping ($P>4$). The gel-like solution structure was able to form below LCST (as evidenced by the above rheological studies), since the interchain association probability was easily beyond the mean-field prediction for gelation threshold, which gave ca. 0.01 ($\sim N^{-1}$).[22] Above LCST, the gel-like network would shrink but the connectivity [the structural strength of the solutions was high enough as shown in Figure 7(b)] allowed uniform shrinkage, which finally resulted in the formation of the sponge-like solid (Figure 5). The sponge-like structure was assumed to be responsible for the fast remixing of PNIPAM. As a result, the streaking effect disappeared.

The endothermic heat from DSC peak area during the demixing transition also confirmed the three regimes (Figure 9). Notably, the endothermic heat exhibited a sharp drop in Regime III. The decrease of the endothermic heat confirmed less chain-water association, since the chain-water association led to heat release. Through the addition of an organic solvent classified as kosmotrope in water, Bischofberger *et al.* confirmed that hydrophobic hydration was the prevailing contribution to control the phase behavior of PNIPAM.[15] In regime III, the sharp drop suggested a great deal of interchain association occurred below LCST, attributing to interchain high overlap ($P>4$ in this regime). Such a great deal of interchain association resulted in the formation of the gel-like structure solution below LCST, as confirmed by the above theological studies.

CONCLUSIONS

The aggregation and dissolution behavior of PNIPAM in water was studied. Interestingly, the DSC results showed three concentration regimes with different phase behavior. In regime I with an upper threshold ca.10 wt %, two remixing peaks at 32.5 and 31.0°C were found in the cooling run. In regime II with an upper threshold ca. 40 wt %, one remixing peak at 29.9°C following the remarkable streaking effect was observed during cooling. However, in regime III with higher than 40 wt % of PNIPAM, the streaking effect disappeared. The optical observation exhibited different phase-separated patterns formed above LCST: colloidal particles in regime I, large precipitates in regime II, and the sponge-like solid in regime III. The light scattering and rheological studies showed that the different solution structures occurred below LCST: free chains and small clusters in regime I, large clusters in regime II, and a gel-like network in regime III. Further studies found that the different regimes arose from their corresponding solution structures below LCST, which was well explained based on the overlapping parameter P. Different solution structures below LCST led to the formation of different phase-separated patterns above LCST that generated different remixing behavior as observed by DSC. Therefore the

two remixing peaks in regime I were derived from the bimodal-distribution colloidal particles formed above LCST, the streaking effect in regime II was due to the large precipitates formed above LCST, and the disappearance of streaking effect in regime III came from the formation of the sponge-like structure above LCST. To summarize, the aggregation and dissolution behavior of PNIPAM strongly depended on the solution structure below LCST. Although our discussion was focused on the relatively low molecular weight fractions, higher molecular weight fractions were expected to show the similar behavior, which warrants future work.

ACKNOWLEDGMENTS

This work was supported by Hubei Co-Innovation Center for Utilization of Biomass Waste, Scientific Research Project of Hubei Provincial Department of Education (Q20102709) and Foshan Innovative and Entrepreneurial Research Team Program (No.2013IT100122).

REFERENCES

1. Schild, H. G. *Prog. Polym. Sci.* **1992**, *17*, 163.
2. Aseyev, V. O.; Tenhu, H.; Winnik, F. M. *Adv. Polym. Sci.* **2006**, *196*, 1.
3. Zhang, G. Z.; Wu, C. *Adv. Polym. Sci.* **2006**, *195*, 101.
4. Wever, D. A. Z.; Picchioni, F.; Broekhuis, A. A. *Prog. Polym. Sci.* **2011**, *36*, 1558.
5. Liu, R.; Fraylich, M.; Saunders, B. R. *Colloid Polym. Sci.* **2009**, *287*, 627.
6. Wever, D. A. Z.; Ramalho, G.; Picchioni, F.; Broekhuis, A. A. *J. Appl. Polym. Sci.* **2014**, *131*, 39785.
7. Wu, C.; Zhou, S. Q. *Macromolecules* **1995**, *28*, 8381.
8. Wu, C.; Zhou, S. Q. *Phys. Rev. Lett.* **1996**, *77*, 3053.
9. Wang, X. H.; Qiu, X. P.; Wu, C. *Macromolecules* **1998**, *31*, 2972.
10. Hsu, S. H.; Yu, T. L. *Macromol. Rapid Commun.* **2000**, *21*, 476.
11. Cheng, H.; Shen, L.; Wu, C. *Macromolecules* **2006**, *39*, 2325.
12. Spěváček, J. *Curr. Opin. Colloid Interf. Sci.* **2009**, *14*, 184.
13. Ding, Y. W.; Ye, X. D.; Zhang, G. Z. *Macromolecules* **2005**, *38*, 904.
14. Ding, Y. W.; Zhang, G. Z. *Macromolecules* **2006**, *39*, 9654.
15. Bischofberger, I.; Calzolari, D. C. E.; De Los Rios, P.; Jelezarov, I.; Trappe, V. *Sci. Rep.* **2014**, *4*, 4377.
16. Gorelov, A. V.; Du Chesne, A.; Dawson, K. A. *Phys. A* **1997**, *240*, 443.
17. Chan, K.; Pelton, R.; Zhang, J. *Langmuir* **1999**, *15*, 4018.
18. Aseyev, V.; Hietala, S.; Laukkanen, A.; Nuopponen, M.; Confortini, O.; Du Prez, F. E.; Tenhu, H. *Polymer* **2005**, *46*, 7118.
19. Wever, D. A. Z.; Riemsma, E.; Picchioni, F.; Broekhuis, A. A. *Polymer* **2013**, *54*, 5456.
20. Yu, T. L.; Lu, W. C.; Liu, W. H.; Lin, H. L.; Chiu, C. H. *Polymer* **2004**, *45*, 5579.
21. Pamies, R.; Zhu, K. Z.; Kjøniksen, A. L.; Nyström, B. *Polym. Bull.* **2009**, *62*, 487.
22. Rubinstein, M.; Colby, R. H. Polymer Physics; Oxford University Press:, New York, **2003**.
23. Balu, C.; Delsanti, M.; Guenoun, P.; Monti, F.; Cloitre, M. *Langmuir* **2007**, *23*, 2404.
24. Chambon, F.; Winter, H. H. *Polym. Bull.* **1985**, *13*, 499.
25. Winter, H. H. *Polym. Eng. Sci.* **1987**, *27*, 1698.
26. Tanake, H. *J. Phys. Condens. Matter.* **2000**, *12*, R207.
27. Tanaka, H. *Phys. Rev. Lett.* **1996**, *76*, 787.